

## COMBINED PHYSICAL TESTING AND FINITE ELEMENT MODELLING OF FEATURES IN GRAPHITE COMPONENTS

Jona Melia<sup>1</sup>, Samuel Primavesi<sup>2</sup>, Jim Skelton<sup>3</sup>, Mark Kirkham<sup>4</sup>

<sup>1</sup> Mechanical Engineer, Amentum, Manchester, UK (jona.melia@global.amentum.com)

<sup>2</sup> Mechanical Engineer, Amentum, Manchester, UK (samuel.primavesi@global.amentum.com)

<sup>3</sup> Senior NDT Consultant, Amentum, Warrington, UK (jim.skelton@global.amentum.com)

<sup>4</sup> Principal Consultant, Amentum, Warrington, UK (mark.kirkham@global.amentum.com)

### ABSTRACT

In graphite-moderated reactors, such as Advanced Gas-cooled Reactors (AGRs), graphite is used as both structural and moderator material. Numerous material properties of graphite evolve with irradiation, such as Young's Modulus, strength, coefficient of thermal expansion, and thermal conductivity (Campbell et al. (2016)). Graphite also undergoes significant irradiation induced dimensional change over its lifetime. At low dose, graphite undergoes shrinkage. At higher dose, this dimensional change shifts to growth, leading to expansion of the material. In AGRs, this turnaround in dimensional change can cause significant internal stresses, which can be exacerbated by thermal stresses when the reactors are shut down. Additionally, channel distortions result in external loading of components as load is transferred between them. This, combined with the strength reduction due to radiolytic oxidation, can lead to crack initiation of components.

This paper describes how a series of physical tests were carried out in Amentum's laboratories in series with equivalent Finite Element (FE) Analyses to simulate various states of stress in AGR fuel bricks and how, from the combination of the two, critical stresses at which the fuel bricks would be predicted to fail in the reactors can be determined. Ultimately, this work is to support the plant lifetime extension programs for the UK's AGR fleet

Physical tests were carried out using unirradiated graphite on which material characterisation tests were performed. The flexural strengths of the material used in the tests were then compared to that originally used in specific reactors, allowing critical stresses to be calculated for unirradiated graphite typical in each reactor. Further methods not discussed in detail in this paper use this unirradiated critical stress to calculate the irradiated critical stress for the specific reactor. Further scaling factors are then calculated by the graphite user material subroutine (UMAT) in subsequent stress analyses on irradiated/oxidised graphite to determine critical stresses that are relevant to a particular feature, in a particular component, in a particular reactor at a particular time.

## INTRODUCTION

In graphite-moderated reactors, such as the UK Advanced Gas-cooled Reactors (AGRs), graphite is used as both structural and moderator material in the form of reactor core graphite bricks and keys. When subjected to fast neutron irradiation, graphite exhibits dimensional change, and the mechanical and thermal properties progressively change, such as Young's Modulus, strength, coefficient of thermal expansion and thermal conductivity (Campbell et al. (2016)). Further complications include the non-homogeneous nature and complex microstructure of graphite, the combination of which can result in strength tests of graphite coupons not being representative of populations of components, or features within components. Therefore, testing at the scale of specific features or components, which tend to be substantially larger than test coupons, is required to determine specific behaviours. Localised stress concentration initiates crack growth from the keyway root for the fuel and reflector bricks, and from the externally loaded key root for interstitial integral keyed bricks. This can be assessed through finite element modelling of destructive tests.

The reactor core bricks are subject to stresses arising from internal sources and external loading. Internal stresses arise from differential material shrinkage due to an irradiation dose gradient, which in later life of the reactor causes a compressive stress on the inner bore of the bricks and a tensile stress on the outer surface of the bricks. External loading on the keys and keyways arises due to the movement of adjacent bricks caused by the dimensional change-induced brick distortions and other core driving mechanisms.

If the graphite brick columns distort to a degree where insertion of sufficient control rods or cooling of fuel stringers is no longer viable, then safe shutdown or cooling of the reactor would be prevented. Safe shutdown and cooling of the reactor are fundamental nuclear safety requirements, the continuation of which is essential to plant lifetime extension.

The site licensee will use the irradiation, weight loss, strength and other properties as key factors to build their evidence for lifetime extension safety cases. Regulators, such as the Office for Nuclear Regulation (ONR) for the UK nuclear sector, will assess the licensee's safety case.

This paper discusses the unirradiated graphite brick slice tests which have the same key features as the fuel bricks in the Hartlepool/Heysham 1 (HRA/HYA) (Mena et al. (2018)) and Heysham 2/Torness (HYB/TOR) (Davies. M (1996)) reactor cores. The tests determine the critical stresses that arise from internally-generated stresses and externally-generated stresses which are used for calculating the Fractional Remanent Strength (FRS) (McLachlan et al. (1996)). This is a measure of how close a component is to crack initiation at any given time in life under any given Plant Operating Condition.

### ***Critical Stress and FRS***

In this paper, internal and external stress are investigated separately by following the FRS method, developed by EDF Energy (McLachlan et al. (1996)). The failure load gathered from the experimental data were representative for HRA/HYA and HYB/TOR graphite specimens. The experimental failure loads were then implemented into the FE analysis to determine the critical stresses at which cracks will initiate in the brick under reactor operating conditions. The critical stresses can be utilised for material properties inputs in further analyses for determining the FRS (McLachlan et al. (1996)). The FRS is the adopted method for AGR graphite component failure assessments using a deterministic approach and is accepted by the ONR. Assessment codes have been developed around the FRS to enable analysis of structural integrity in specific locations within the graphite core components. In the FRS equation each type of stress is compared with its critical stress, these utilisations are summed together. Traditionally an FRS value of 0.2 has been found to indicate a cracked component, accounting for uncertainty/variability. See FRS in equation 1 below (Sarkar et al. 2024):

$$\Delta S = 1 - \left[ \frac{\sigma_S}{M_I \sigma_{crS}} + \frac{\sigma_T}{M_I \sigma_{crT}} + \frac{\sigma_P}{M_I \sigma_{crP}} + \frac{\sigma_L}{M_L G K \sigma_{crL}} \right] \quad (1)$$

Where

- $\Delta S$  is the FRS,
- $\sigma_S$  is the calculated shrinkage stress,
- $\sigma_{crS}$  is the critical stress for shrinkage,
- $\sigma_T$  is the calculated thermal stress,
- $\sigma_{crT}$  is the critical stress for thermal stress,
- $\sigma_P$  is the calculated pinching stress,
- $\sigma_{crP}$  is the critical stress for pinching,
- $\sigma_L$  is the calculated load applied stress,
- $\sigma_{crL}$  is the critical stress for external loading,
- $M_I$  is the material bulking factor for internal stress,
- $M_L$  is the material bulking factor,
- $G$  is the geometric bulking factor,
- $K$  is the key tilt factor.

### ***Previous Work***

The programme of test rigs presented in this paper determines the appropriate critical stresses for use in graphite brick stress analyses which was developed from similar work carried out in the 1990s. For this paper, the rig tests to simulate the external loads on the fuel bricks were an improvement on previous work carried out on both HRA/HYA and HYB/TOR fuel brick geometries.

The internal stresses of a graphite bricks in the reactor core cannot be replicated directly. Instead, an analogous external load must be applied to simulate internal stress. For the internal stress test rig, the original design from previous work applied both a bending moment and a compressive load to part of the graphite slice. The improved method for this paper's test rig used long levers to minimise the compressive force for a given bending moment. Digital image correlation (DIC) for specimen alignment and detailed strain maps to better validate the corresponding FE analyses was also implemented using the method described by Gill et al. (2021).

Additionally, in the previous work, there were no measurements of the strength of the parent material being tested, so it was not known whether the components evaluated were weaker or stronger than the typical graphite brick located in the reactors. In contrast, in this work the flexural strength of the material used in these tests were characterised through four-point bend tests; the Dynamic Young's Modulus and density measurements were also obtained.

## **PHYSICAL TEST METHODOLOGY**

### ***Graphite Specimen***

For the internal stress test rig, three graphite brick slices were used; HRA/HYA interstitial keyway, HYB/TOR interstitial keyway and HYB/TOR loose keyway slices, these are shown in Figure 1. Two HYB/TOR slice geometries were used to ensure that both capacities for the interstitial and loose keyways were determined. The HYB/TOR loose keyway specimen only used one keyway as the interstitial keyway is weaker which would prohibit the replication of internal stress at the loose keyway. Only one geometry for HRA/HYA was needed as the interstitial and loose keyways are identical. The internal test specimens were adapted from their fuel brick geometries, with only the regions around the specific keyways in question being analysed to aid the replication of internal stresses.

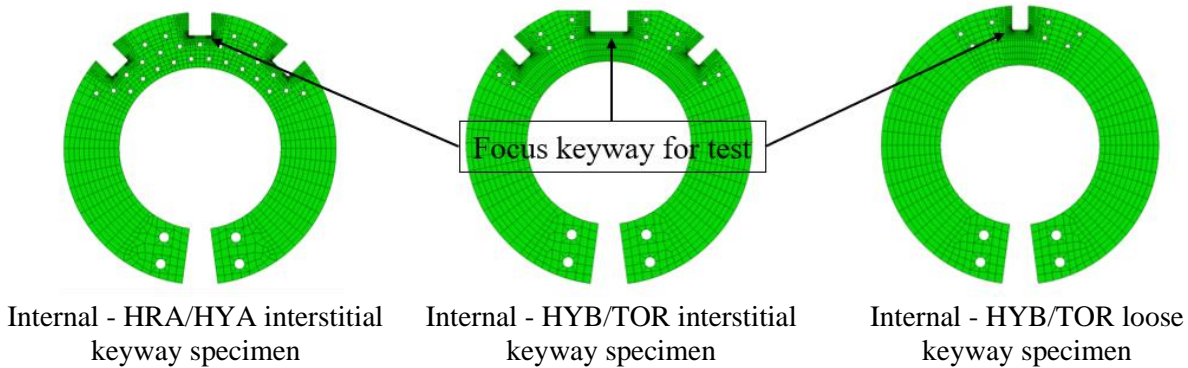


Figure 1. Internal test rig specimens.

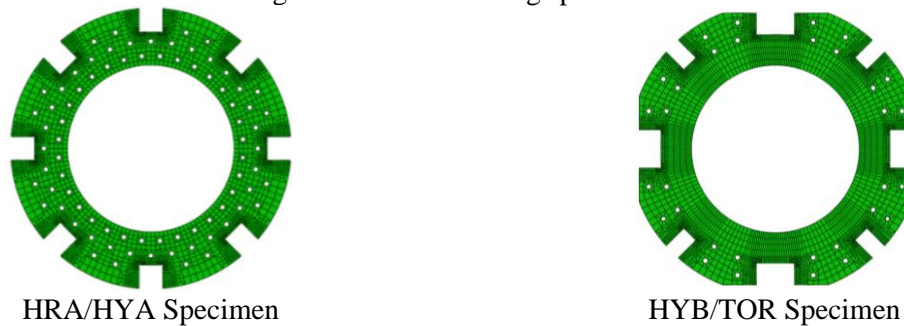


Figure 2. External test rig specimens.

The graphite specimens used in the external load tests were representative of fuel bricks used in the reactor, featuring all keyways and methane holes, these are shown Figure 2.

### ***Internal Load Test Method***

The internal load test rig, shown in Figure 3 (Left), comprises the graphite specimen bolted to two long levers, one moving and one static. Between the lever ends a linear actuator applies a tensile load until failure. Displacements were recorded during the tests using five Linear Variable Differential Transformers (LVDTs). Two strain gauges (SGs) were used to record strain in the bore adjacent to the prominent keyway.

The main output from the internal test was the load applied at the lever end at failure. The test also provided the internal brick displacements and the crack initiation location of the specimen. The failure load was used as the loading conditions to be applied to the FE models. The recording of displacements and strains also provided a means of validating the FE model against the physical test rigs.

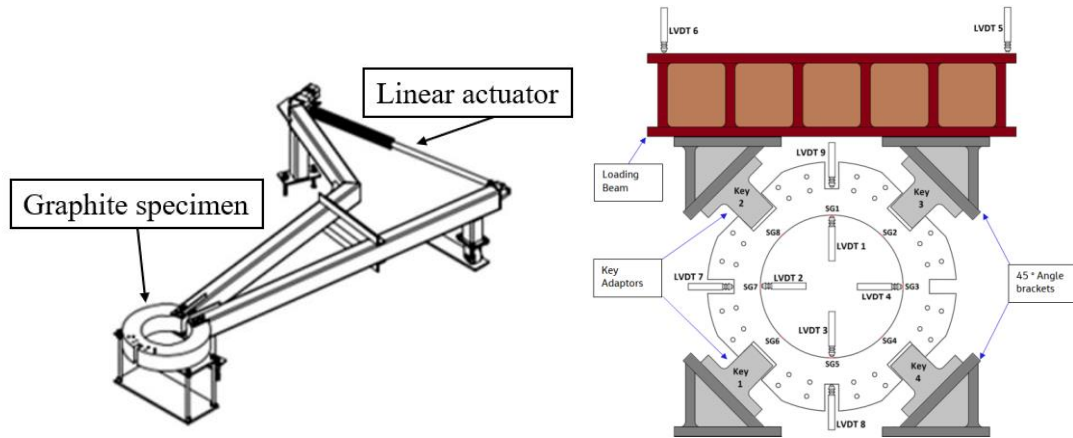


Figure 3 – (Left) Schematic of the internal stress test rig with HRA/HYA specimen and (Right) schematic of external test rig with a HYB/TOR specimen loading in the interstitial keyway.

### *External Load Test Method*

The external load test rig, shown in Figure 3 (Right), was designed to apply the load to failure of one of four radial keyways (either the loose or interstitial) around the external circumference of a fuel brick slice, placing the brick slice into tension or compression depending on the loading direction. For each fuel brick geometry (HRA/HYA and HYB/TOR), two forms of tests were carried out to simulate tensile and compressive loading, this was done for loading in the interstitial keyways and repeated for the loose keyways.

As can be seen in Figure 3 (Right), the north-east, south-east, south-west and north-west keyways were loaded by key adaptors, which is a single component for the interstitial keyway configuration and a combination of a key and a key mounting bracket for the loose keyway configuration. Two adaptors were attached to the loading beam and two to the frame bedplate via 45° angle brackets. The loading was applied vertically upwards or downwards through the upper loading beam, this method replicates the external loading the graphite brick would experience within the reactor. Displacements were recorded during the tests using nine LVDTs, and eight SGs which were used to record the strain distribution in the bore.

In addition, DIC was used to get detailed displacement and strain maps of the brick slices throughout the tests, using the method described by Gill et al. (2021). DIC was implemented using a speckled pattern being applied to the two planar surfaces of the specimen before the loading took place. This consisted of a base coat of white paint followed by black paint speckles applied via aerosol spray. This results in a pseudo-randomly distributed pattern with high greyscale contrast.

Load train alignment for these tests was crucial for applying the load uniformly to the various keyways. Figure 4 shows DIC-based alignment check results. Figure 4 (Left) is a well-aligned tension test, the small arrows pointing upward implies very little specimen rotation. Conversely, Figure 4 (Right) shows a poorly aligned compression test, with the arrows showing the specimen rotation.

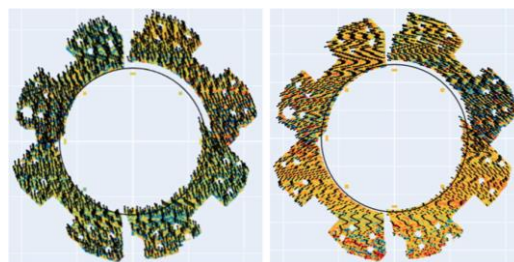


Figure 4. Example of well aligned DIC-measured displacements (Left) and poorly aligned (Right)

## MODELLING TECHNIQUES

The FE model's mesh was made of quadratic elements with the mesh refinement in the keyway root replicating previous work so that the critical stress comparisons would be valid. The specimens and their corresponding meshes can be seen in Figure 1 for internal stress cases and Figure 2 for external load cases.

The internal stress test rig was reproduced in ABAQUS (Dassault Systemes, 2024) as a beam representation with a solid body graphite brick slice, shown for HRA/HYA in Figure 5. To load the model with the same approach as the test arrangement, a force was applied between the ends of the two long levers. The load was generated at the beams which represented the two end nodes of the levers. The magnitude of the load applied in ABAQUS was the mean load to failure of the experimental rig tests.

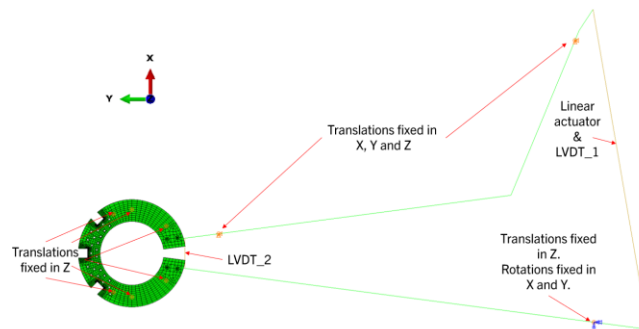


Figure 5. Diagram of the internal stress Finite Element model, showing the HRA/HYA specimen.

The external load case was modelled using Abaqus (Dassault Systemes, 2024), as shown for HYB/TOR in Figure 6. The FE model comprised of solid body representation of the steelwork and graphite specimens. The steel key brackets, loose keys and loose key mounting brackets were all modelled for replicating the rig test. Quadratic elements were used for the fuel brick slice, keys and mounting brackets. The loading beam and angle brackets above the specimens in the test rig were sufficiently rigid, the load was applied as a concentrated force to a reference point which was linked to the top surfaces of the brackets through rigid connectors (including no rotation). The magnitude of the loads applied was the mean load to failure of the experimental tests carried out.

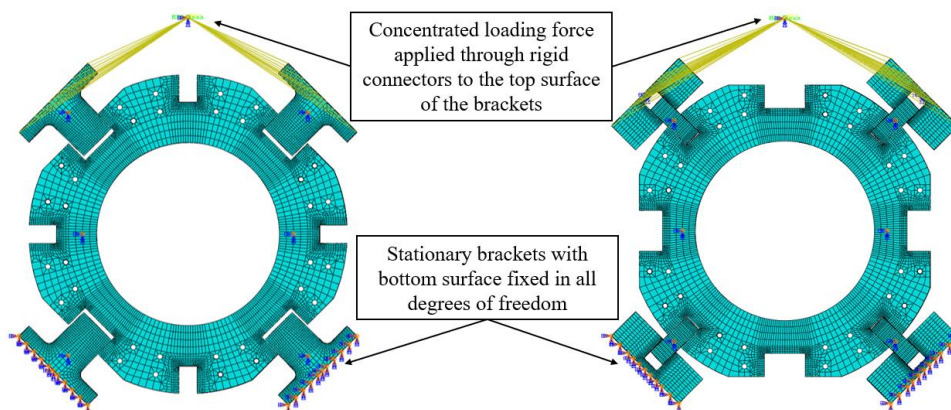


Figure 6. Examples of FE models of the external load tests, showing HYB/TOR (Left) interstitial tensile and (Right) loose compressive.

## RESULTS

### *Specimen Behaviour in Test Rig*

The test rig specimens each cracked at the root of one of the keyways, as expected. In the internal stress test rig, the location of failure was biased to the left side of the loaded keyway, which was the side connected to the moving lever of the rig, as shown in Figure 7 (Left) for a HRA/HYA specimen. Only three of the twelve specimens tested failing at the root on the right side of the loaded keyway. For the HRA/HYA specimen, the crack propagated towards and across the closest methane hole before reaching the bore. In the two HYB/TOR specimens, cracks would propagate from the root of the loaded keyway straight through to the bore.

For the external load tests, the behaviour of the specimens depended on the direction of loading (i.e. tension or compression) but was consistently seen in the form of a crack propagating at a 45° angle from the keyway root to the bore surface. Figure 7 (Right) shows that for a HRA/HYA specimen (in this case under a tension) the crack propagated across the methane holes. The compressive interstitial keyway load case produced crack propagation in the opposite side of the South West keyway, again travelling upwards towards the bore. The loose keyway under tension loading had crack growth in the South West keyway, and for compression loading the crack growth was in the North East keyway.

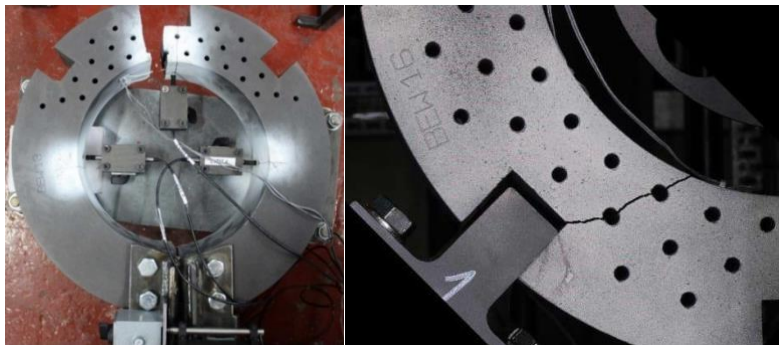


Figure 7. Examples of failed specimens on the (Left) internal stress test rig and external stress test rig for an interstitial keyway under a tension load (Right).

### *Comparison to Finite Element Analysis Results*

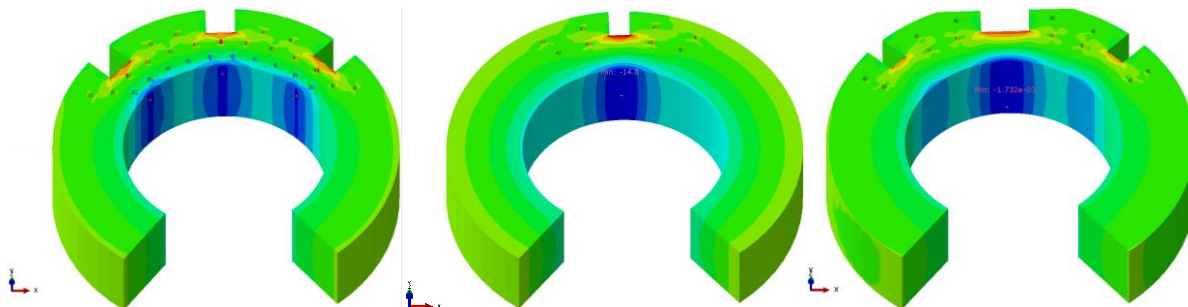


Figure 8. Left - Contour plot of hoop strain in the bore in the HRA/HYA interstitial Keyway specimen.  
Middle - Contour plot of hoop strain in the bore in the HYB/TOR loose Keyway specimen.  
Right - Contour plot of hoop strain in the bore in the HYB/TOR interstitial Keyway specimen.

The difference between the FE analysis and experimental data results for the internal load tests have been documented in Table 1. For the internal tests, the diameter changes and strain gauge values had strong agreement between the FE and experimental results. In the FE models, the keyways with high stress build up also had crack growth in the experimental tests, see Figure 8 for the FE hoop strain plots with strain build up in the keyway roots.

Table 1. Internal stress test comparison between FE tests and experimental results

Specimen	% Difference between FE analysis and Experimental data		
	LVDTs at failure	Bore Diameter Change	Bore Strain
HRA/HYA	26.7	-14.4	-9.2
HYB/TOR interstitial Keyway	24.9	-8.9	-11.4
HYB/TOR loose Keyway	47.3	-6.6	-10.6

The internal load FE model had highest stress close to the keyway root, where the failure was seen in the rig tests. For most of the specimens, the load at lever end was uniform until failure with similar gradients to the FE models. The HYB/TOR loose keyway experiments had slightly less consistent gradients for the BEX14 experiment as this was data from the rig during commissioning before small modifications.

Example plots of vertical bore diameter change and a SG plot for external load FE results and the experimental load results have been documented in Figure 9. The vertical bore diameter change was gathered using the LVDTs in the rig and the corresponding locations in FE were used to extract the displacement values. By examining the change in bore shape in the vertical direction and the strain gauges located in specified locations on the specimen, a clear similarity in stiffness between the rig data and FE results can be seen, Test B vertical bore change result was removed due to an LVDT functioning incorrectly.

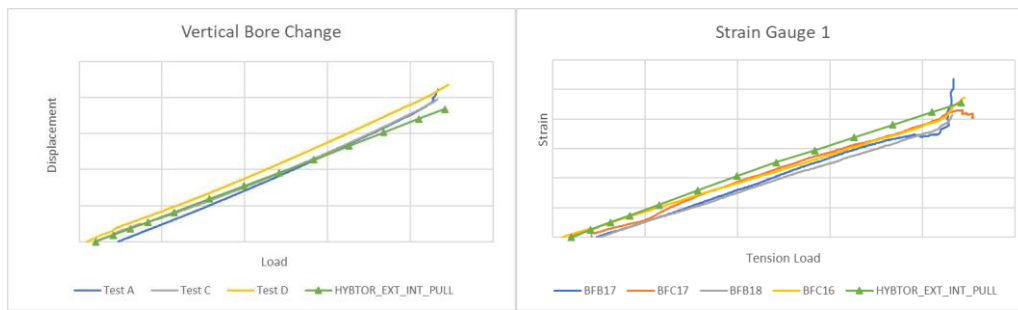


Figure 9 - FE results vs experimental data for the HYB/TOR interstitial keyway with external tension load being applied.

### *Young's Modulus Investigation for Internal Stress FE analysis*

A supplementary analysis was carried out to consider the effect of variation in the applied Young's Modulus (9-12 GPa) for the internal stress specimen. Figure 10 shows the maximum principal stress in each of the six keyways in the HRA/HYA specimen for each of the applied values of Young's Modulus. As expected, the plot shows that there was negligible change in the peak maximum principal stress seen in the keyway roots when the Young's Modulus was changed, since the model was loaded by a prescribed force, rather than a prescribed displacement. This investigation validated the assumption that, even without perfect agreement of displacements and strains within the specimen the peak principal stresses did not vary with

changed Young's Modulus values. Hence the critical stress would not differ for the graphite specimens with a variance in Young's Modulus being applied.

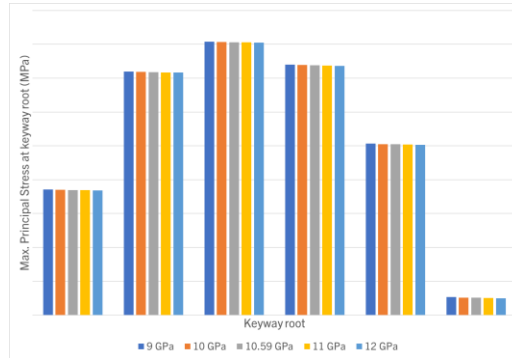


Figure 10. Maximum principal stress in the keyway roots of the HRA/HYA specimen at different applied values of Young's Modulus.

### Scaling approach

Basic material four-point bend tests were carried out for the graphite material at selected positions of each source brick or billet used for the component tests discussed above. By scaling the mean flexural strength of the material used in the physical tests to that of the unirradiated graphite used in the reactors, the peak stresses found in the FE models can be scaled according to Equation (2).

$$\tilde{\sigma}_{cr} = \sigma_{cr} \cdot \frac{f_r}{\bar{f}_b} \quad (2)$$

Where

- $\tilde{\sigma}_{cr}$  is the scaled critical stresses for the original, unirradiated graphite in each of the reactors,
- $\sigma_{cr}$  is the critical stress gathered using the FE model of the specimens in the rig test,
- $\bar{f}_b$  is the mean flexural strength of the material in the billets of graphite,
- $f_r$  is the flexural strength of the original, unirradiated graphite in each of the reactors.

## DISCUSSION AND CONCLUSIONS

In the UK AGR fleet, the graphite keys and keyways connect adjacent bricks, providing structural rigidity. Stress concentrations form at the roots of these keyways which can result in crack initiation, the focus of lifetime extension safety cases. The critical stress is the stress at which the graphite component will crack at the keyway root under a particular loading condition (e.g. internal shrinkage stress). The FRS uses the calculated critical stresses to evaluate whether a graphite component will crack at the keyway root at a given stress state.

When a stress analysis is carried out on irradiated graphite, a material model calculates factors to further scale the critical stress to account for the effects of irradiation and oxidation. These factors are applied to provide an irradiated critical stress that is relevant to the location in the component and dose of the component at that time.

The methodology in this paper can be applied to calculate unirradiated graphite critical stresses, which can then be used to calculate irradiated graphite critical stresses. These critical stresses support assessments that provide an accurate evaluation of the state of brick integrity in the reactor core, enabling safe operation and lifetime extension.

The ability to combine the physical testing experiments with the FE analysis is a key aspect for continued assessment of graphite brick integrity for the lifetime extension programmes of AGRs. Building on previous experiments, with the use of material characterisation tests on smaller specimens and combining with FE analysis enables understanding and evaluating the graphite brick integrity within the core.

## ACKNOWLEDGEMENTS

The authors would like to thank EDF Energy Generation for their support in funding these tests. Their contribution made the analyses possible, and we greatly appreciate their commitment to advancing this work. The views expressed are those of the authors, and not necessarily those of EDF Energy Generation.

## REFERENCES

- Campbell, A. A, Katoh, Y., Sead, M. A. and Takizawa, K. (2016). Property changes of G347A graphite due to neutron irradiation. *Carbon*, Volume 109, Pages 860-873
- Dassault Systemes, Abaqus , (2024). Retrieved from: <https://www.3ds.com/products-services/simulia/products/abaqus/> [Accessed 20/01/2025]
- Davies, M. W. (1996). Graphite core design in UK reactors (pp. p. 47–56.).
- Gill, P, Onwuarolu, P, Smith, R, Coult, B, Kirkham, M, Sutcliffe, M, Cooper, K, Schofield, T, Madew, C, McLennan, A, & Currie, C. (2021). "A Method for Investigating Multi-Axial Fatigue in a PWR Environment." *Proceedings of the . Volume 1: Codes and Standards*. Virtual, Online. V001T01A012. ASME. <https://doi.org/10.1115/PVP2021-62429>
- McLachlan, N, Reed, J, and Metcalfe, M P. (1996). *AGR core safety assessment methodologies*. IAEA. Page 131
- Mena, J, Edmondson, P, Margetts, L, Griffiths, D, Windes, W, Carroll, M, Mummery, P. (2018). Characterisation of the spatial variability of material properties of Gilsocarbon and NBG-18 using random fields. *Journal of Nuclear Materials*. 511. 10.1016/j.jnucmat.2018.09.008.
- Sarkar, S, Jennings, R, Davies, M and Primavesi, S. (2024). "Applicability of AGR graphite models and assessment methods for HTGR applications", The 7th EDF Graphite Conference, Manchester, UK.